

Interface properties and valence-band discontinuity of MnS/ZnSe heterostructures

L. Wang and S. Sivananthan

Microphysics Laboratory, Physics Department, University of Illinois at Chicago, 845 West Taylor Street, Chicago, Illinois 60607-7059

R. Sporken and R. Caudano

Laboratoire Interdisciplinaire de Spectroscopie Electronique, Facultés Universitaires Notre-Dame de la Paix, Rue de Bruxelles 61, 5000 Namur, Belgium

(Received 12 February 1996; revised manuscript received 1 April 1996)

Tetrahedrally bonded, metastable zinc-blende single-crystalline, single-phase MnS was grown by molecular-beam epitaxy on ZnSe buffer layers grown on GaAs(100) substrates. The interface between MnS and ZnSe was studied by transmission electron microscopy and x-ray photoelectron spectroscopy. The valence-band discontinuity in β -MnS/ZnSe heterostructures was measured by x-ray-induced photoelectron spectroscopy. The valence-band discontinuity is not resolved in valence-band spectra from the interface, thereby implying that it is small. We therefore determined the discontinuity from the separation of the core levels at the interface and in reference samples of ZnSe and β -MnS. The results indicate that the valence-band discontinuity at the β -MnS/ZnSe interface is small (about 150 meV) and that the band alignment is of type II. This result agrees with low-temperature photoluminescence measurements on MnS/ZnSe superlattices. [S0163-1829(96)02727-0]

INTRODUCTION

Lattice-matched quantum-well structures based on the quaternary alloy $\text{Zn}_{1-x}\text{Mn}_{1-y}\text{Se}_x\text{S}_y$ could be a possible alternative to the Mg-based materials for laser or light-emitting diode applications in the blue-green region of the visible spectrum. This system replaces the highly chemically reactive Mg with less reactive Mn, reducing the ionicity of the material while offering similar possibilities for a wide range of wide-gap quaternary alloys lattice matched to GaAs or ZnSe. In heterostructures, the electronic transport properties are determined, to a large extent, by the electronic structure near the interfaces. The purpose of this paper is to describe the structure of the interface between MnS and ZnSe and reports on an experimental study of the valence-band discontinuity between these materials. This information is critical for calculating the electronic band structure of the quaternary structures.

MnS is a semimagnetic semiconductor with a large band gap ($E_g = 3.8$ eV at 0 K). During equilibrium growth techniques, MnS crystallizes in the stable rocksalt phase. The metastable tetrahedral zinc-blende or wurtzite phases of MnS have been prepared mainly by low-temperature chemical synthesis or evaporation techniques. Okajima and Tohda have reported the direct growth of MnS by gas source molecular-beam epitaxy (MBE) onto GaAs (100), (111)A, and (111)B oriented substrates. At substrate temperatures between 150 °C and 250 °C single-crystalline wurtzite MnS was grown on (111) oriented substrates while similar growth on GaAs(100) substrates yielded a mixture of zinc-blende, rocksalt, and wurtzite phases.¹ Recently, we have grown single-crystal zinc-blende MnS on GaAs(100).^{2,3} However, we found that the direct exposure of GaAs to S causes interfacial roughness,^{2,3} in agreement with observations by Guha *et al.*⁴ We speculated that this could be due to a chemical reaction involving the formation of volatile Ga_2S .⁵ Simi-

larly, MnSe and MnTe were grown as single-crystalline layers with the zinc-blende structure by MBE.^{6,7} This has been achieved even though for MnS, MnSe, and MnTe the stable structure is the rocksalt structure when prepared by equilibrium growth methods.⁸

EXPERIMENT

All samples for this work were grown on GaAs(100) substrates MBE in a RIBER 2300 system at University of Illinois at Chicago. This MBE chamber is connected to two surface analysis chambers through transfer modules and hence the samples can be transferred between the growth chamber and the analysis chambers through ultrahigh vacuum. For a comprehensive description of the growth, we refer the reader to previous publications.^{2,3} Briefly, the GaAs substrates were chemically etched in a 4:1:1 solution of $\text{H}_2\text{SO}_4:\text{H}_2\text{O}_2:\text{H}_2\text{O}$, rinsed in HCl and H_2O and then loaded into the UHV system. The native oxide was desorbed *in situ* by heating the substrate to about 600 °C. Once the desorption was complete, the substrate is cooled down with Zn or Se flux and the ZnSe growth initiated at 350 °C using elemental Zn and Se. The corresponding growth rate was 0.1 nm/s.

MnS was grown using a conventional effusion cell for Mn and a cracker cell for sulfur. Since the GaAs surface reacts with elemental sulfur, exposing it to a flux of sulfur would make it rough. Therefore, MnS was not grown directly on GaAs, but only on top of the ZnSe grown on GaAs. The growth rate was in the range of 0.05–0.1 nm/s and the substrate temperature was set to 100 °C to 125 °C. The low growth temperature is necessary to maintain the zinc-blende structure. Our study shows that zinc-blende MnS can be grown on ZnSe/GaAs with a thickness of more than 50 nm. This is much beyond the information depth for x-ray-induced

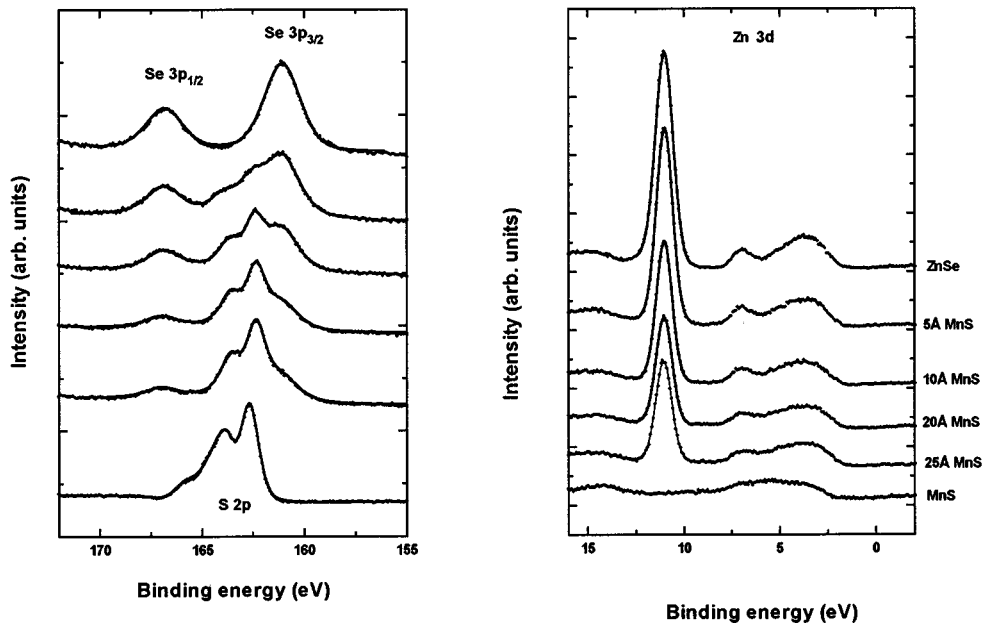


FIG. 1. XPS spectra from (a) the Se $3p$ and S $2p$ core levels and (b) the Zn $3d$ core level and valence band. The spectra are for a thick layer of ZnSe(100) on GaAs, β -MnS(100) on ZnSe(100)/GaAs(100) with increasing MnS thickness, and a thick layer of MnS(100) on ZnSe(100)/GaAs(100), respectively. The dots are the experimental data; the solid line is a fit of the core levels as explained in the text.

photoelectron spectroscopy (XPS).

For the XPS measurements, we used an SSX-100 instrument with a monochromatic and focused Al $K\alpha$ x-ray source and a hemispherical analyzer with constant pass energy. In this work, we used a spot size of $300\ \mu\text{m}$ diameter and a pass energy of 25 eV, which results in a nominal resolution of 700 meV. The binding energies are measured with respect to the Fermi level, which was calibrated from the Au $4f$ lines (83.9 eV).

RESULTS AND DISCUSSION

For ZnSe grown on GaAs(100) we have measured double-crystal x-ray rocking curves with a full width at half maximum as low as 27 arc sec and free exciton linewidth of 0.93 meV in the photoluminescence (PL) spectra at low temperature.² Both values confirm the high degree of structural perfection of the layers and show that the growth of ZnSe by MBE is optimized. β -MnS was then grown on such ZnSe layers and the growth interrupted several times to record photoelectron spectra.

Figure 1 shows a series of typical spectra recorded for different thickness of MnS on ZnSe. The left panel shows the Se $3p$ and S $2p$ doublets, while the right panel shows the Zn $3d$ doublet and the valence band. The topmost spectrum on each panel is from a thick layer (about 350 nm) of ZnSe on GaAs(100). The lowest spectrum on each panel is from a 30-nm-thick layer of β -MnS on ZnSe/GaAs. In between these two end points, we show typical spectra for various thin layers of β -MnS on ZnSe/GaAs. Similar spectra were obtained on other samples.

These spectra were analyzed by fitting them to the sum of several spin-orbit split doublets with mixed Gaussian-Lorentzian line shape, added to a Shirley-type background. For a given core level, the same spin-orbit parameters were used for the whole range of MnS thickness. The result of this fit is shown by the solid line that is superimposed on the experimental data. We find that the Se $3p$ and Zn $3d$ spectra

could be fitted to a single doublet for all samples. Upon the first deposition of MnS (0.5 nm), these peaks shift to slightly lower binding energy (0.1–0.15 eV), due to different band bending; a subsequent increase of the MnS thickness does not alter their position. The S $2p$ spectra can be fitted to a single spin-orbit split doublet, except for the 30-nm-thick layer of β -MnS. For the thin layers, the binding energy decreases slightly (about 150 meV) with increasing thickness. For the 30-nm-thick layer, the S $2p$ spectrum is fitted to the sum of two doublets of mixed Gaussian-Lorentzian line shape. The strongest doublet is located at 162.66 ± 0.05 meV (S $2p_{3/2}$) and is due to emission from S in MnS. This is about 300 meV higher than the S $2p_{3/2}$ peak from the 2-nm-thick layer. A much weaker doublet near 164 eV, is due to elemental sulfur at the surface. This additional S is probably due to the S flux maintained on the sample during the initial cooldown after growth.

The Mn $3p$ core levels are shown in Fig. 2. These core levels are recorded in the same spectral window as the Se $3d$ peaks. Although a meaningful analysis of their line shape is difficult, changes in binding energy can be extracted easily from the spectra. By comparing two different procedures we have obtained very reproducible results. First, we determined the position of the Mn $3p$ core level from the half-width point at half height. This was done after subtracting either a linear base line or a Shirley-type background. Next, we fitted the spectrum to a single peak of mixed Gaussian-Lorentzian line shape. The center of this peak follows the position of the half-width point at half height within 50 meV. We emphasize again that this is only a way of determining the change of the peak position rather than an analysis of the line shape. With this procedure, we find the position of the Mn $3p$ peak to be independent of the MnS thickness, except for the 30-nm-thick layer, for which the Mn $3p$ peak follows the S $2p$ one. For the valence band, no striking new features are observed at any stage of the growth. Instead, the MnS valence band progressively replaces the one from ZnSe. We conclude that there is no significant reaction at the

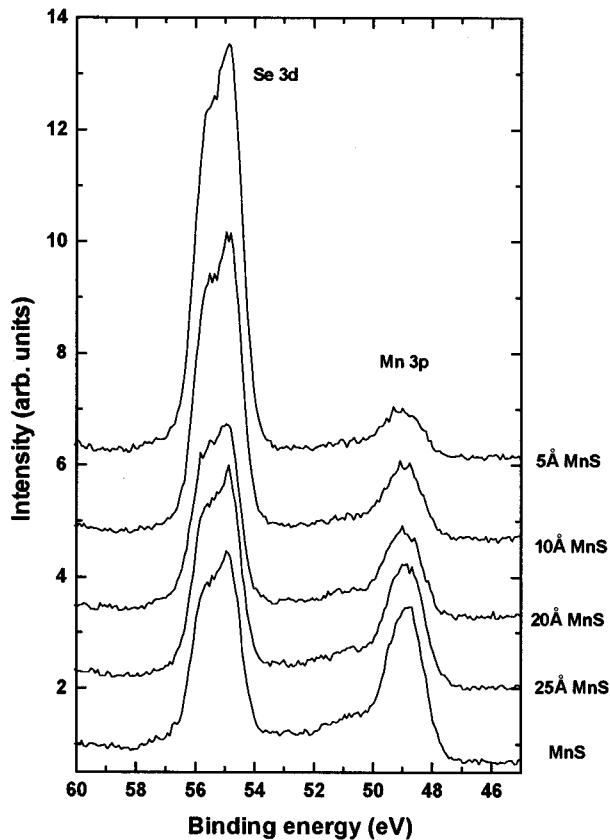


FIG. 2. XPS spectra from the Se 3d and Mn 3p core levels. The spectra are for β -MnS(100) on ZnSe(100)/GaAs(100) with increasing MnS thickness and for a thick layer of MnS(100) on ZnSe(100)/GaAs(100).

ZnSe/MnS interface. At least, for thin layers and within the resolution of our spectrometer, we do not detect any of the elements in a different electronic environment than the pure binary compounds. Only the S peak position changes slightly as a function of MnS thickness, suggesting that the interface formation starts with the adsorption of sulfur. As we have pointed out before, the elemental sulfur on some of the thicker layers seems to be due to adsorbed species rather than to interface reactions. Such a peak is not seen on thin layers. The variation of the various peak areas as a function of the MnS thickness is compared in Fig. 3 with a calculation based on exponential attenuation of the photoemission signals through a uniform overlayer. The peak areas were determined from the peak fitting procedure described before, except for Mn 3p, where numerical integration was used after subtracting a Shirley-type background. An average over several samples yields effective attenuation lengths of 2.2 nm (Zn 3d), 1.9 nm (Se 3p), 1.7 nm (S 2p), and 2.0 nm (Mn 3p), respectively. These values were obtained from a least-squares fit of the calculated curves to the experimental peak areas. Although some deviation is observed between the experimental points and the calculated curves, the values for the effective attenuation length are quite reasonable. This shows that although the MnS layer may not grow in a perfectly two-dimensional fashion, departure from the two-dimensional growth should be very limited, since unrealistically small values would be obtained for the attenuation

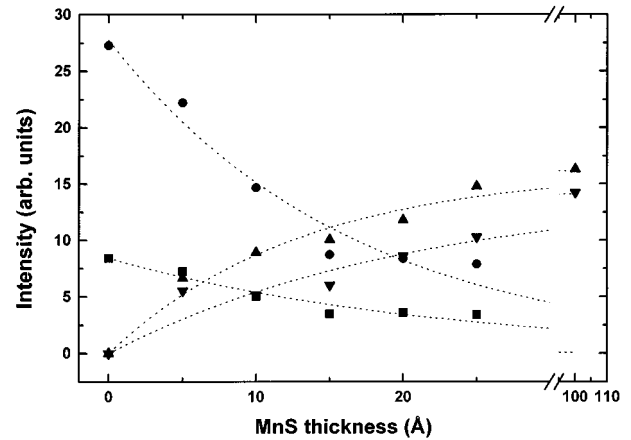


FIG. 3. Se 3p (●), S 2p (▲), Mn 3p (▼), and Zn 3d (■) peak areas determined as described in the text. For the S 2p, the contribution from elemental sulfur has been subtracted. The dashed lines are fits based on an experimental attenuation of the photoemission signals through a uniform overlayer.

length in the case of three-dimensional growth. These results also confirm that the interface with ZnSe is reasonably abrupt. The deviations between the experimental points and the calculated curves can be attributed to the numerous simplifying assumptions in the analysis of the area versus thickness curves.

High-resolution transmission electron microscopy (TEM) also shows that well-ordered interfaces are obtained and that interface roughness or intermixing is limited to about 2 or 3 ML.⁹ This should be considered an upper limit and is consistent with the XPS results. Due to the similarity between the two binary compounds, such a limited deviation from a perfectly abrupt interface cannot be detected by XPS. TEM also confirms that both the MnS and ZnSe grow in the zinc-blende structure.

We now use the XPS data to determine the valence-band discontinuity at the β -MnS/ZnSe interface. The valence-band spectra do not resolve the valence-band discontinuity directly. This implies that the discontinuity is small and that we have to use an indirect procedure¹⁰ based on the separation between core levels (Fig. 4). The separation between a core level and the valence-band maximum is measured for each of the binary compounds. These numbers along with the separation of these same core levels at the interface allow us to obtain the valence-band discontinuity between β -MnS(100) and ZnSe(100) according to

$$\Delta E_V = (E_V - E_{CL})_{\text{MnS}} - (E_V - E_{CL})_{\text{ZnSe}} + \Delta E_{CL}. \quad (1)$$

The maximum of the valence band in the binary compounds was taken as the intercept between a linear fit of the leading edge in the photoelectron spectrum and a horizontal background (Fig. 5). A better approach would be to compare the measured spectra to a theoretical density of states,¹¹ but such a calculation is not available for β -MnS at this time.

The peak positions were determined by least-squares peak fitting, except for Mn 3p, where we used the half-width point at half height. When the interface is formed, the binding energy of the core levels can change due to chemical shift or due to band bending. To determine the valence-band

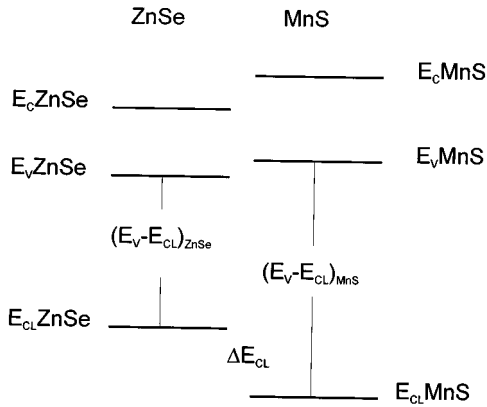


FIG. 4. Schematic energy-band diagram for the ZnSe/MnS interface and of the method used to determine the valence-band discontinuity.

discontinuity, we need to remove possible contributions from chemical shift and only take into account contributions from band bending.¹² Based on the behavior of the core levels that we have described, we assume that only the S core levels are

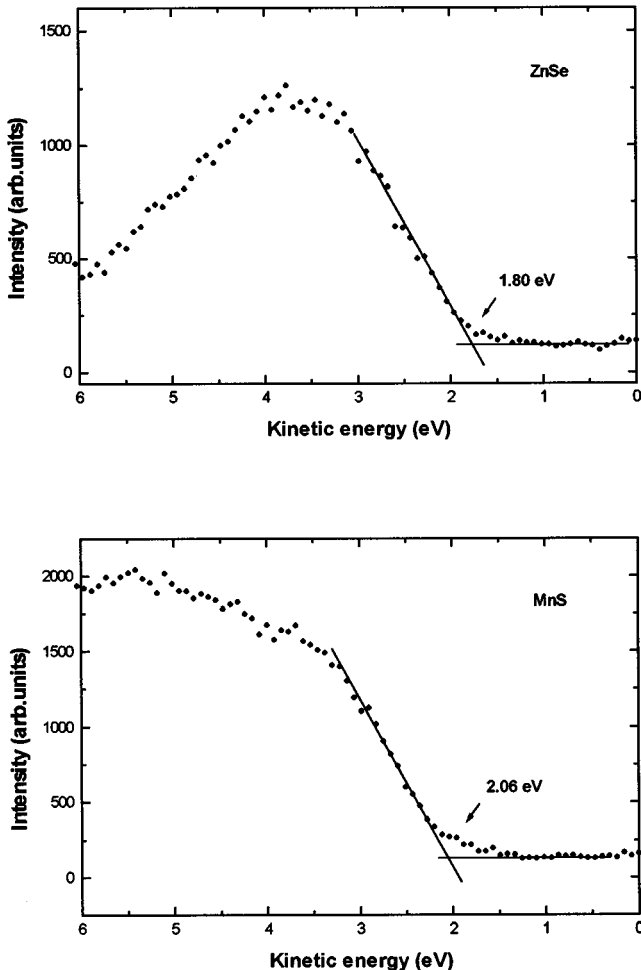


FIG. 5. Determination of the valence-band maximum of ZnSe(100) and β -MnS(100) by linear extrapolation of the leading edge in the spectrum.

affected by a weak chemical shift, whereas the Zn, Se, and Mn core-level positions change only due to band bending. We therefore use the pairs of core levels Zn 3*d*–Mn 3*p* and Se 3*d*–Mn 3*p*. We find that the valence-band discontinuity between ZnSe(100) and β -MnS(100) is 0.15 ± 0.10 eV, regardless of which of these combinations of core levels we choose and independent of the MnS thickness. According to our experiment, the valence-band maximum of ZnSe is below that of MnS. Since the band gaps of ZnSe and β -MnS are 2.82 and 3.8 eV, respectively, this means that the band alignment is of type II.

The uncertainty on the valence-band discontinuity is related mainly to the accuracy with which we can locate core levels and valence-band maxima in the spectra. The accuracy is related to the resolution of our spectrometer and to the validity of the procedure, i.e., the description of the spectra in terms of background, line shape for the core levels and linear extrapolation for the valence-band maximum. The validity of linear extrapolation cannot be assessed quantitatively because too little is known about the band structure of β -MnS. However, this method has been quite successful in the past for other II-VI semiconductor heterojunctions.¹² For MnS, we also mentioned that elemental sulfur is present on some of the thicker layers that were used to measure the separation between the Mn 3*p* core level and the valence-band maximum. This should have only little effect on the measurement, since we expect only little contribution from the elemental sulfur near the top of the valence band, based on the relative intensity of the two S 2*p* doublets. In a separate experiment, we have grown several samples of β -MnS, where the S flux was cut off at different times during the cool-down. The results confirmed that the elemental sulfur appears at the surface during the cool-down. Moreover, we do not observe an effect of the elemental sulfur on the measured separation $(E_V - E_{CL})_{MnS}$. As for the separation between core levels, we estimate that they result in an uncertainty of ± 50 meV on the valence-band discontinuity, based on a comparison of data from various samples and different combinations of core levels and based on the experience with our peak fitting software. Changes of the valence-band discontinuity (sample to sample, effect of growth conditions, etc.) can thus be measured with about 50-meV accuracy, whereas we estimate the accuracy of the absolute value of the discontinuity to be about 100–150 meV.

Strain could also affect the determination of the valence-band discontinuity based on Eq. (1). Indeed, the separation between the core levels and the maximum of the valence band was measured on relaxed layers of the binary compounds, while the separation between the core levels at the interface corresponds to layers with a variable degree of strain, depending on the thickness of the MnS layer. We expect this effect to be small because the lattice mismatch between β -MnS and ZnSe is small (about 1%). In principle, such effects can be predicted theoretically.¹³ However, since not enough is known about the effect of strain on the electronic structure of β -MnS, such a calculation is not obvious in the present case. In similar experiments, other authors have found that at least in some cases, the valence-band discontinuity is affected by strain much less than what is predicted theoretically and does not seem to depend on the de-

tails of the electronic structure of the overlayer.^{14,15} Also, the separation between the Zn, Se, and Mn core levels does not depend on the thickness of the MnS layer, which suggests that the effect of strain is less than the accuracy of the XPS measurements.

In summary, we find that the valence-band discontinuity between ZnSe(100) and β -MnS(100) is 0.15 ± 0.10 eV, with a type-II band alignment. Taking the uncertainty of these measurements into account, the valence-band discontinuity could also be close to zero, but we can certainly rule out a large discontinuity with a type-I alignment. This result is confirmed by low-temperature PL measurements on MnS/ZnSe superlattices.^{2,9} Near band-edge PL spectra were measured on an eight-period superlattice with 3-nm-thick β -MnS layers alternating with 5- to 6-nm-thick ZnSe layers on a 0.17- μ m-thick ZnSe buffer on GaAs(100). A peak near 2.77 eV is observed, which is about 50 meV below the bulk band gap of ZnSe. Since such a peak is not seen on bulk ZnSe, we tentatively assign it to electrons in the ZnSe buffer layer and holes in (probably the first) MnS layer of the superlattice. This would imply a type-II band alignment with a valence-band discontinuity of about 50 meV, which is in reasonable agreement with the XPS results. We also note that no peaks are observed above the band gap of ZnSe, while this could be expected in the case of a type-I alignment.

CONCLUSION

We have grown MnS/ZnSe heterostructures on GaAs(100) by MBE. Under optimum conditions, metastable zinc-blende MnS on ZnSe/GaAs(100) has been grown by MBE, with a thickness of more than 50 nm. Both TEM and XPS show that intermixing or interface roughness is limited to a few monolayers. The valence-band discontinuity at the interface between MnS and ZnSe was measured by XPS. We find a small discontinuity, of about 150 meV, and a type-II band alignment. This is confirmed by low-temperature PL measurements on a MnS/ZnSe superlattice.

ACKNOWLEDGMENTS

We would like to thank J. P. Faurie for stimulating discussions, D. J. Smith for the TEM work, B. Skromme for the PL measurements, and Z. Ali for expert technical assistance. This work was supported by National Science Foundation under Contract No. NSF ECS 9202664 and by a NATO collaborative research travel grant. R.S. acknowledges support from the Belgian Fund for Scientific Research (FNRS).

¹M. Okajima and T. Tohda, *J. Cryst. Growth* **117**, 810 (1992).

²B. J. Skromme, Y. Zhang, D. J. Smith, and S. Sivananthan, *Appl. Phys. Lett.* **67**, 2690 (1995).

³B. J. Skromme, Y. Zhang, W. Liu, B. Parameshwaran, D. J. Smith, and S. Sivananthan, in *Growth, Processing, and Characterization of Semiconductor Heterostructures*, edited by G. Gumbs, S. Lieryi, B. Weiss, and G. W. Wicks, MRS Symposia Proceedings No. 326 (Materials Research Society, Pittsburgh, 1994), p. 15.

⁴S. Guha, B. J. Wu, H. Cheng, and J. M. DePuydt, *Appl. Phys. Lett.* **63**, 2129 (1993).

⁵D. A. Andrews, R. Heckingbottom, and G. J. Devies, *J. Appl. Phys.* **54**, 4421 (1983).

⁶W. Heinbrodt, O. Goede, I. Tschentscher, V. Weinhold, A. Klimakow, U. Pohl, K. Jacobs, and N. Hoffman, *Physica B* **185**, 357 (1993).

⁷S. M. Durbin, J. Han, S. M. Kobayashi, D. R. Menke, R. L. Gunshor, Q. Fu, N. Pelekanos, A. V. Nurmikko, D. Li, J. Gon-salves, and N. Otsuka, *Appl. Phys. Lett.* **55**, 2087 (1989).

⁸O. Goede and W. Heimdrodt, *Phys. Status Solidi B* **146**, 11

(1988).

⁹S. Sivananthan, L. Wang, R. Sporken, J. Chen, B. J. Skromme, and David J. Smith, *J. Cryst. Growth* **159**, 94 (1996).

¹⁰S. P. Kowalczyk, E. A. Kraut, J. R. Waldrup, and R. W. Grant, *J. Vac. Sci. Technol.* **21**, 482 (1982); J. R. Waldrop, R. W. Grant, S. P. Kowalczyk, and E. A. Kraut, *J. Vac. Sci. Technol. A* **3**, 835 (1985).

¹¹E. A. Kraut, R. W. Grant, J. R. Waldrup, and S. P. Kowalczyk, *Phys. Rev. B* **28**, 1965 (1983).

¹²A. D. Katnani, R. R. Daniels, Te-Xiu Zhao, and G. Margaritondo, *J. Vac. Sci. Technol.* **20**, 662 (1982).

¹³Tran Minh Duc, C. Hsu, and J. P. Faurie, *Phys. Rev. Lett.* **58**, 1127 (1987); R. Sporken, S. Sivananthan, D. Ehlers, J. Fraxedas, J. J. Pireaux, L. Ley, R. Caudano, and J. P. Faurie, *J. Vac. Sci. Technol. A* **7**, 427 (1989).

¹⁴C. G. Van de Walle, K. Shaszad, and D. J. Olego, *J. Vac. Sci. Technol. B* **6**, 1350 (1988).

¹⁵R. S. List, J. C. Woicik, I. Lindau, and W. E. Spicer, *J. Vac. Sci. Technol. B* **5**, 1279 (1987).